

Torque planning errors affect the perception of object properties and sensorimotor memories during object manipulation in uncertain grasp situations

Abbreviated title: Torque planning errors bias object perception

Author Names and Affiliations: Thomas Rudolf Schneider^{1*}, Gavin Buckingham², Joachim Hermsdörfer¹

¹ Chair of Human Movement Science, Department of Sport and Health Sciences, Technical University of Munich, Georg-Brauchle-Ring 60/ 62 D-80992 Munich, Germany

² Sport and Health Sciences, College of Life and Environmental Sciences, University of Exeter, Heavitree Road, EX1 2LU, Exeter, UK

* **Corresponding Author:** Thomas Rudolf Schneider, Thomas.Rudolf.Schneider@tum.de

Keywords: object manipulation, grasping, sensorimotor prediction, torque perception, weight perception, motor error

1 Abstract

Predicting instead of only reacting to the properties of objects we grasp is crucial to dexterous object manipulation. While we normally plan our grasps according to well-learned associations, we rely on implicit sensorimotor memories when we learn to interact with novel or ambiguous objects. However, little is known about the influence of sensorimotor predictions on subsequent perception and action. Here, young and elderly subjects repeatedly lifted an object in which the center of mass was randomly varied between trials straight upwards with the aim to prevent object tilts. After each lift, subjects indicated the location of the perceived center of mass and reported how heavy the object felt. Surprisingly, we found that sensorimotor torque memories eventually causing initial lifting errors had substantial effects on the perception of torques, weight, and the torque planning for the next lift. Whereas subjects tended to partly retain their previous erroneous sensorimotor memories (instead of solely relying on the previously encountered torque for the upcoming motor plan), they perceived encountered torques stronger when they erroneously predicted them. Additionally, we found that torque prediction errors, as well as the actual torques made the object feel heavier. By contrast, perception did not influence upcoming motor control. There were no major differences observed between the age groups. The sensorimotor impact on torque perception can be explained by internal feedforward prediction highlighting task-relevant errors while the partial retention and adaptation of sensorimotor torque memories is reconciled with the trial-to-trial learning rule for motor adaptation.

2 New & Noteworthy

The current study is the first to demonstrate in an object manipulation task in uncertainty that errors in the sensorimotor prediction of torques influence perception of both torques and weight, whereas sensorimotor torque memories are partly retained and partly adapted to planning errors. Our results

24 provide novel insights into the predictive mechanisms underpinning the common everyday task of
25 object manipulation and further support theories about the predictive modulation of perception
26 established in other neuroscientific disciplines.

27 **3 Introduction**

28 To grasp and manipulate objects, the incorporation of predicted object properties into a motor plan is
29 crucial to reduce initial motor errors before sensory feedback becomes available and is processed.

30 While a myriad of learned object representations can be accessed through visual cues like size
31 (Gordon et al. 1991), geometry (Fu and Santello 2012), material (Buckingham et al. 2009), object
32 identity (Hermsdörfer et al. 2011) or arbitrary cues (Ameli et al. 2008), action planning relies on
33 object dynamic representations acquired in recent lifts in the absence of informative visual cues.

34 These so called ‘sensorimotor memories’ are quickly and unconsciously learned to guide force
35 (Johansson and Westling 1984) and torque programming (Lukos et al. 2013) on a trial-to-trial basis.

36 In addition to shaping the motor plan, internal models are also believed to underpin dynamic forward
37 models by creating predictions of the expected sensory states arising from the execution of the motor
38 plan (Wolpert and Flanagan 2001). By comparing the predicted and the actual sensory input, the CNS
39 monitors the action progress and allows for updating of the internal models. In addition, feedforward
40 predictions of sensory states based on an efference copy of the motor plan have been shown to shape
41 perception by dampening the perception of self-induced action consequence (von Holst 1950). This
42 phenomenon, which presumably exists to highlight externally-caused sensory events, has been
43 demonstrated for eye movements and finger-tip force production (for reviews see: Franklin and
44 Wolpert 2011; Wolpert and Ghahramani 2000).

45 Studies investigating the interplay of motor prediction and perception in object manipulation yielded
46 surprising findings: In studies in which subjects had to grasp equally heavy objects of different sizes

47 (Flanagan and Beltzner 2000) or surface material (Buckingham et al. 2009) subjects only initially
48 scaled force rates according to object size or material and quickly harmonized force rates while they
49 persistently judged the lighter-looking object to feel heavier. These findings were interpreted as
50 evidence that these weight illusions were not induced by mismatches of sensorimotor prediction, but
51 rather by violated weight expectations, highlighting the independence of hedonic perception and the
52 control of action. (Flanagan and Beltzner 2000).

53 Recently however, a pioneering study by (van Polanen and Davare 2015) showed that in the absence
54 of visual cues to object weight, subjects who lifted a light object after having lifted a heavy object
55 over-scaled their force rates and also perceived the lifted object as feeling lighter. This was regarded
56 as the first evidence of an effect of sensorimotor prediction mismatches on weight perception.
57 Furthermore, effects of the mass distribution (Amazeen and Turvey 1996) and the grip force levels
58 (Flanagan and Bandomir 2000; Flanagan et al. 1995) were shown to affect the heaviness perception.

59 To our knowledge, no previous research has investigated the interplay between errors in torque
60 prediction and perception in a basic object manipulation task. Here, by having subjects lift a neutral
61 object with an unforeseeably varying center of mass, inevitably torque planning errors occur at lift
62 onset. We assess the effect of these on torque and heaviness perception to evaluate whether
63 prediction errors have a task specific or even a generalized effect on perception. We hypothesize that
64 torque planning errors add to torque perception in the direction of the error and furthermore increase
65 the heaviness percepts. Regarding the heaviness perception, we additionally test whether torques per
66 se add to heaviness perception.

67 Although previous studies of torque prediction in uncertain situations have shown that torques at lift
68 onset partly resemble the previous trial's affordance (Lukos et al. 2013), it is unclear whether
69 sensorimotor predictions are also partly retained. Based on the trial-to-trial learning rule for motor

adaptation (Gonzalez Castro et al. 2014), we predicted that previous sensorimotor predictions still influence performance on upcoming trials, biasing the upcoming torque prediction towards the previous prediction. Furthermore, we explored if conscious perception influences action planning beyond the encountered physical properties, and controlled our findings for unspecific error-reducing delay strategies. To date, no study has yet investigated the age dependency of torque prediction and perception. As groups of young and elderly participants participated in the study, we additionally explored whether these mechanisms are age dependent.

4 Materials and Methods

4.1 Participants

Overall 24 participants, consisting of 12 young (5 female, 7 male, all right-handed, 18-28 years, mean age 22.8 ± 3.4 years) and 12 elderly (5 female, 7 male, 10 right-handed, 2 left-handed, 62-76 years, mean age 69.0 ± 4.9 years) individuals with normal or corrected to normal vision took part in the experiment. Handedness was assessed by self-report. All subjects were naïve to the purpose of the study and gave informed consent to participate in the experiment. The experimental procedures were approved by the Institutional Review Board of the Technical University of Munich and were in accordance with the Declaration of Helsinki. All subjects had no history of neurological disorders or musculoskeletal disorders of the involved upper limb and were not under the influence of centrally acting drugs. The participants received a small monetary compensation for their participation in the experiment which lasted ~1.5 hours.

4.2 Experimental Design and Statistical Analyses

4.2.1 Experimental Task and -Procedure and the Experimental Apparatus

Subjects were asked to reach, grasp, lift and replace a custom made, inverted T-shaped grip device originally introduced by (Fu et al. 2010) (see Figure 1 A) consisting of a vertical handle element which was attached over the center of a horizontal bar. The longish grasp surfaces were covered with fine grain sandpaper (Bosch, P320) and allowed subjects to freely choose digit placement. The aluminum panels underneath the grasp surfaces were attached to 6-axis force/torque-sensors (see Data recording below for details) which were concealed from sight. The horizontal bar element contained 5 cavities in which a matching 250 g aluminum weight was randomly positioned prior to each trial. The view of the weight-cavities (and thus the weight distribution of the object) was blocked by a detachable aluminum lid during the trials. A lightweight magnetic position/orientation-tracker (see Data recording below for details) was mounted on top of the horizontal bar. The handle- and bar element each weighed 250 g, resulting in a total object weight of 750 g including the aluminum weight. For each aluminum-weight-position, we calculated the center of mass (CoM) along the horizontal axis in relation to the center line of the grip device and the resulting external torques around a sagittal line through the center with SolidWorks 2014 (Dessault Systems). With negative signs denoting a CoM on the left and accordingly a resulting counter-clockwise external torque, the arising torques amounted to -0.210 Nm, -0.105 Nm, 0 Nm, 0.105 Nm and 0.210 Nm and a respective CoM of -28.4 mm, -14.2 mm, 0 mm, 14.2 mm and 28.4 mm for the weight being placed in the outer left, middle left, center, middle right and outer right cavity (see figure 1B). Subjects used the needle of a digital caliper which was parallel to the horizontal bar and aligned with the right edge of the bar to indicate the perceived center of mass (see figure 1A).

To raise the expectation that total object weight might vary during the course of the experiment, the experimenter initially showed a set of 2 aluminum and 2 plastic weights to the participants and stated that each and any combination of these could be randomly placed in the 5 concealed cavities of the

114 horizontal bar prior to each trial. Subsequently, all weights were hidden from view throughout the
115 experiment and only one aluminum weight was actually used.

116 To assure exact alignment with the caliper, the experimenter exactly repositioned the grip device
117 within the marked boundaries on a mousepad at the beginning and after each grasp-to-lift trial before
118 perceptual judgments were made. To guarantee a comfortable limb posture for grasping, we allowed
119 the subjects to initially position and orient the apparatus at their discretion by shifting the underlying
120 mousepad.

121 The subjects were instructed to reach for the grasp-device with their dominant hand after the first
122 signal tone, grasp it at the grasp surfaces with the fingertips of the thumb-, index- and middle finger
123 and lift it in a natural, not hesitant, movement while preventing the object to tilt to the side. Subjects
124 were aware that they could freely position their fingers on the grasp surfaces while avoiding the
125 edges. Subjects were asked to hold the object at a height of ~10-15 cm until a second tone 4 seconds
126 after the first signaled them to replace the device.

127 Consequently, subjects should indicate where along the length of the object it could be balanced
128 without tilting (i.e., the center of mass), with the caliper. Then, subjects were asked to give the
129 numerical value that they felt best represented the heaviness of the object they had just lifted. No
130 constraints were placed on this value or its range other than larger numbers representing heavier
131 weights (i.e., absolute magnitude estimation) (Zwislocki and Goodman 1980). After each trial,
132 subjects were asked to close their eyes while the experimenter relocated the aluminum weight (even
133 when the weight position remained the same by chance, the weight was removed and reinserted).
134 Care was taken to ensure that participants could neither visually nor acoustically infer the position of
135 the weight. Overall, each subject lifted the device 100 times and hereby encountered each weight
136 configuration 20 times. The position-sequence was randomly determined for each participant

137 independently employing the ‘datasample’ function in Matlab 2016a (MATLAB,
138 RRID:SCR_001622) beforehand.

139 **4.2.2 Data Recording**

140 The forces and torques exerted on both sides were recorded by two 6-axis force/torque sensors (ATI
141 Nano-17 SI-50-0.5, ATI Industrial Automation; force range: 50,50, and 70 N for x-, y-, and z-axes,
142 respectively; force resolution: 0.012 N; torque range 0.5 Nm; torque resolution: 0.063 Nmm,
143 sampling rate 200 Hz) and digitally converted and transferred to a laptop by a Net-F/T-Transducer-
144 box (ATI Industrial Automation). A magnetic tracker (TrakSTAR, Ascension Technology
145 Corporation, accuracy: 1.4 mm RMS, 0.5 degrees RMS, sampling rate 200 Hz) was fixed centrally
146 on the top of the horizontal base to digitally record the position and orientation of the device. Data
147 collection was synchronized using custom software written in Matlab 2012 (MATLAB,
148 RRID:SCR_001622).

149 **4.2.3 Data Processing and Task mechanics**

150 Data processing and analysis were conducted with custom software written in Matlab 2016a
151 (MATLAB, RRID:SCR_001622). After data collection, the force/torque data was filtered through a
152 sixth-order Butterworth low-pass filter with a cutoff frequency of 14 Hz.

153 The crucial time point of lift onset, corresponding to the moment when sensory feedback about object
154 weight and weight distribution becomes available, was defined as the moment 10ms prior to which
155 the vertical position of the object raised above a threshold of 0.2 mm.

156 We examined the following variables: (1) grip force (GF) was defined as the mean force acting
157 orthogonal against the grasp surfaces, (2) load forces (LFs) were directed upwards on each side of the
158 handle. The center of pressure (CoP) was defined as the vertical distance of the mean center of

pressure of the forces applied on each side relative to the sensor reference point and (3) ΔCoP was defined as the difference between the right and the left CoP. Note, that the CoP of the index-and middle finger side relates to a virtual finger combining index and middle finger while the separate positions as well as forces exerted by the two fingers are unknown. (4) The total exerted torque is comprised of two torque components: (a) the torque generated by the product of the side difference between the load forces and half the distance between the grasp-surfaces and (b) the product of the mean grip force and ΔCoP (For details on the task mechanics and the calculation of the CoPs and torques see supplementary Figure S1). To have the exerted torques match in sign with the external torques they compensate for, all clockwise exerted torques were defined as negative and all counter-clockwise torques as positive. The torque exerted at lift onset, prior to sensory feedback about the external torque, is considered a valid indicator of motor torque prediction (Fu et al. 2011; Fu and Santello 2012; Fu et al. 2010; Zhang et al. 2010). The difference between the external torque and the exerted torque is the uncompensated torque corresponding to the net torque acting on the grip device which causes a rotational acceleration after lift onset. We coin the difference between the external torque and the exerted torque at lift onset planning error (5) (planning error = external torque – torque at lift onset) as indicator of the success of motor torque prediction. As a measure of the task consequence of the planning error before corrections have taken place (Zhang et al. 2010), we measured the peak object tilt in the frontal plane in the first 300ms after lift onset (6). To account for the individual variation in the hesitancy of lift execution, we subject-wise Z-standardized the time from the initial contact of the grasp surfaces until lift onset. The aforementioned variables are illustrated in the representative trial depicted in Figure 2.

4.2.4 Data Management

Due to technical errors 1.5% (35/2400) of the measurements were faulty and the respective observations were discarded. The reported heaviness estimates were subject-wise Fischer z-

transformed. The raw caliper values conferred from the digital display were centered to the grip center. It was evident that while some subjects tried to give physically reasonable judgments, others projected their perception of mass asymmetry to the full scale of the caliper ([-106 mm, 106 mm]) although the real center of mass varied across a notably closer range ([-28.4 mm, 28.4 mm]) and it is physically impossible to encounter an object which entire mass is concentrated in its edges (see supplementary Figure S7). Therefore, the stated CoMs reflect individual representations of perceived torques to the caliper range, rather than a physical representation of the center of mass. To further focus on this individual representation, we Z-standardized the CoM indications subject-wise. As the object CoM and the resulting torques can be converted and are identical after Z-standardization, we refer to the perceived torque in the following, as torque is the physical quality which can actually be perceived by grasping. The pattern of CoM judgments of participant 4 who alternately declared the CoM to be either on the far left or the far right (see supplementary Figure S7), irrespective of the actual CoM, clearly deviated from all other participants and was deemed unreasonable. As Participant 4 lacked both German and English language fluency, it is possible that this participant did not fully understand the instructions regarding the CoM judgment. Hence, we excluded participant 4 from the analysis of perceived torques. Regarding the heaviness perception, some subjects judged the object to be extraordinary light during the first few trials (see supplementary Figure S10). Some subjects reported their surprise about the low weight of the metal surfaced object. As the obvious surprise effect quickly mitigated and distorted the otherwise rather linear time trend, we excluded all heaviness ratings which were 2.5 SD above or below the mean. It was evident that the majority of the subjects considerably varied in their heaviness rating indicating that they perceived weight differences. The statistical models for the exerted torque at lift onset included experimental variables from the previous trial as predictors. As these were missing for the first trial and for each trial following an observation discarded due to technical errors, we had to discard these trials for model

207 fitting. After data cleaning, the datasets contained 2310 observations for the exerted torque at lift
208 onset-model, 2265 observations (23 subjects) for the perceived torque (Z-score)-model and 2329
209 observations for the perceived weight (Z-score)-model.

210 **4.2.5 Statistical Analysis**

211 All statistical analyses were conducted in the R environment for statistical computing (version 3.5.0,
212 (R Core Team 2018), R Project for Statistical Computing, RRID:SCR_001905).

213 Prior to model building, we inspected scatterplots of the response variables against trials and the
214 proposed predictors to judge whether ‘trial’ should be included as predictor and if the relations
215 between the other predictors and the responses were indeed linear.

216 To simultaneously test our hypotheses represented by continuous and categorical predictors which
217 hereby control for each other, we chose a multiple linear regression modelling approach. As we were
218 interested in the within person fluctuation of motor prediction and object perception and not person
219 means, we centered raw predictor variables which varied from trial to trial at the individual subject’s
220 mean. Hence, these variables represented the within person variation (WP) (Hoffman 2014).

221 As we conducted 100 trials per subject, the repeated measurements from each individual cannot be
222 assumed to be independent as observations from one person tend to be more similar than
223 observations between subjects, which may lead to a pronounced inflation of the alpha-errors (Aarts
224 et al. 2014). Therefore, we employed linear mixed effects modelling (LMM). In addition to
225 estimating the group effects like classical linear multiple regression models, the so-called fixed
226 effects in LMM, LMM can also estimate how much these predictor effects vary among the randomly
227 selected subjects around the group effects. By including these so-called random effects for predictors
228 whose effect significantly vary among subjects, LMM accounts for the nesting structure of the data

and safeguards against anti-conservative inference (Aarts et al. 2014; Bates et al. 2000; Long 2011). While the fixed effects/ group effects are included according to the research hypotheses and constitute our main research interest, random effects serve to test the significance of the fixed effects appropriately. The appropriate selection of random effects to include in the model is a controversial statistical issue. To keep the model inferences as conservative as possible but without over identifying the model, we adapted a model building approach described by (Bates 2015). In short, starting with the inclusion of all possible random effects, we first iteratively simplified the random effects structures until they were accommodated by the data. Subsequently, we iteratively tested if the remaining random effects significantly contributed to model fit employing Likelihood-ratio-tests between the more complicated candidate model and the simplified candidate model. Random effects not contributing to model fit were eliminated. As seen for the 'perceived torque' model, it is also possible that none of the found group effects significantly vary among participants so that the model can be simplified to a classical multiple linear regression model.

All LMMs were fitted with the restricted maximum likelihood criterion using the 'lme4' package (R package: lme4, RRID:SCR_015654, (Bates et al. 2015)). The age groups were dummy coded as 0 and 1, so that interactions of the main effects with the age category represent the difference in the main effect between age groups. We will report the findings for both age groups coded as reference group separately. P values of the fixed effects were obtained by Wald-type t-tests with Satterthwaite's method for approximating degrees of freedom as implemented in the 'lmerTest' package ((R package: lmerTest, RRID:SCR_015656)(Kuznetsova et al. 2016)). We screened for violations of the model assumptions with diagnostic plots assessing the linearity of the predictor effects and model predictions as well as the normality of the residuals and the individual random effects estimates and did not detect worrisome deviations. We further report the standardized β -

regression estimates and their respective confidence intervals of significant predictors which were extracted with the ‘sjstats’-package (Lüdtke 2018).

The partial effect plots of the significant effects containing 95% prediction intervals derived from parametric bootstrapping of the final models together with conditional partial residuals were computed with the ‘visreg’-package (Breheny and Burchett 2017). All plots were created with the ‘ggplot2’ package (Wickham 2016) (ggplot2, RRID:SCR_014601) and the modifications introduced in the ‘cowplot’ package (Wilke 2017). As an overall measure of goodness of fit, we report pseudo- R^2 statistics for the fixed effects and random effects of LMMs computed with the ‘piecewiseSEM’ package (Lefcheck 2016) which follows the procedure described in (Nakagawa and Schielzeth 2013) and the R^2 statistic for the classical multiple linear model. Pseudo- R^2 values, analogous to the R^2 measure in classic multiple linear regression, approximate how much of the overall response variance is explained by the model.

4.2.5.1 Modelling the Exerted Torque at Lift Onset

The exerted torque at lift onset was regarded a valid proxy of the sensorimotor memories guiding torque planning, as feedback about the actual external torque is only available after lift onset. We fit two complementary models whose sets of predictors allow us to test different hypotheses. As the external torque equals the sum of the exerted torque at lift onset and the torque planning error (i.e. the difference between the external torque and the exerted torque at lift onset), two of the three above-mentioned predictors must be included in a regression model and the meanings and interpretations of each depends on the other. Regarding overall model prediction, both models lead to virtually equal predictions. In the first model, we included the previous external torque and previous torque planning error. Hence, the coefficient of the previous external torque indicates the degree to which current torque prediction reflects the object properties at the last trial, while the coefficient of the previous

275 planning errors is informative about the role of previous sensorimotor memories relative to the actual
276 previous torque on upcoming torque prediction. The planning error can be envisaged as vector
277 pointing from the exerted torque at lift onset towards the external torque (see Figure 2). While a
278 positive correlation coefficient of the previous planning error would indicate a shift of the torque at
279 lift onset towards the previous external torque, a negative sign would indicate a shift at lift onset
280 towards the previous erroneous torque at lift onset. A coefficient which did not differ from zero
281 would provide no evidence against the assumptions that the CNS fully discards previous
282 sensorimotor memories in favor of a plan which only incorporates previous object dynamics.
283 However, a negative coefficient would indicate that the torque prediction is shifted towards the
284 previous sensorimotor plan, reducing the alignment of the motor plan with the previous task
285 dynamic, while a positive sign would suggest that the previous erroneous plans are not only
286 discarded but even reversed, hence leading to a better alignment with the previous task dynamic than
287 if no error was made. The first model allows us to compare our findings with previous object
288 manipulation studies (e.g. (Lukos et al. 2013)).

289 In force-field-perturbation studies, the trial-to-trial learning rule for motor adaptation (reviewed in
290 (Gonzalez Castro et al. 2014; Ingram et al. 2011)) is a conventional motor learning model which
291 assumes that the states of a sensorimotor memory of object dynamics are partly retained and partly
292 adapted according to the experienced prediction error: $x(n + 1) = \alpha * x(n) + \beta * e(n)$, where $x(n)$ is
293 the state of the model on trial n , α is the retention coefficient, β is the adaptation-rate, and e is the
294 error given by the difference between the perturbing force and the model state. Hence, by including
295 the previously exerted torque at lift onset as a proxy of the previous state of sensorimotor memory,
296 and the previous planning error as a proxy for the sensed prediction error, the respective coefficient
297 of the previously exerted torque at lift onset is informative about sensorimotor retention while the
298 regression coefficient of the previous planning error is informative about the degree to which an

adaptation of the previous sensorimotor model towards previous task dynamics has occurred, with a positive sign denoting adaptation towards the previous external torque.

This analysis allows us to compare our findings with studies employing inconsistently changing force-fields (Gonzalez Castro et al. 2014).

Both models also included the ‘perceived torque (Z-score) at the previous trial’, to test for an effect of conscious perception on action, the ‘external torque at the current trial’, to control for unspecific corrections, as well as the ‘age group’ and the ‘contact to lift onset time (Z-score)’ as fixed main effects. Furthermore, the models contained the interactions of the aforementioned predictors with the age category as well as the all possible two- and three-way interactions among the ‘external torque at the current trial’, the ‘contact to lift onset time (Z-score)’ and the ‘age group’. The exploratory plots suggest no trial effect (see supplementary Figure S2) and rendered the assumption of a linear relation between the predictors and the response as reasonable (see Figure S3). The necessary random effects were separately determined such that the final first LMM contained the random variances of the Intercept, the current external torque, the ‘planning error at the previous trial’, the ‘external torque at the previous trial’ and the ‘perceived torque (Z-score) at the previous trial’, while for the second LMM the ‘Intercept’, and the slopes of the ‘torque at lift onset at the previous trial WP’, the ‘planning error at the previous trial WP’, the current external torque and the ‘contact to lift onset time (Z-score)’ were considered as necessary independent random effects.

4.2.5.2 Modelling the Perceived Torque (Z-score)

The exploratory plots suggest no trial effect (see supplementary Figure S8) and rendered the assumption of a linear relation between the predictors and the response as reasonable (see Figure S9). During the mixed effects model building process all tested random effects were deemed unnecessary as they did not improve model fit. Therefore, the final model was a classical multiple linear

regression model with the ‘perceived torque (Z-score)’ as dependent variable and the ‘external torque’ and ‘planning error WP at the current trial’ as well as their interaction as the predictors chosen for confirmatory hypothesis testing. Additionally, the main effect of the ‘age group’ and the interactions between the other predictors and the ‘age group’ were included.

4.2.5.3 Modelling the Perceived Weight (Z-score)

The scatterplot of the weight percepts across trials (see supplementary Figure S10) suggests a linear trial trend after the exclusion of outliers. The non-parametric ‘loess’-regression curves overlaid over the scatterplots of the weight percepts across the external torque and the planning error (see Figure S11) resemble parabolas. Therefore, we included the trial-number, the linear terms of the external torque and the planning error WP and age group as well as the quadratic terms of the external torque and planning error WP as fixed main effects. Like before, the model further contained the main effect of age group and all fixed interaction effects with age group. Our final model included the subject specific independent random effects of the linear and quadratic effect of the external torque and the linear term of the planning error as well as the covariance between the random effects of the aforementioned linear terms.

5 Results

5.1 Predictive Torque Control: Exerted Torque at Lift Onset

In the present study the peak object tilt was highly correlated with the planning error at lift onset (Pearson’s $R^2 = 0.84$) demonstrating the behavioral importance of the planning error measure.

In the first model the negative Intercept (young: -0.012 [Nm], $t(22.0) = -2.709$, $p = 0.013$); elderly: -0.018 [Nm/Nm], $t(22.0) = -4.054$ [Nm], $p = 0.000528$) suggests that subjects tend to exert a small clockwise torque at lift onset when the external torques and the torque perception are centered and no

prediction error had occurred. The exerted torque at lift onset is positively correlated with the
 external torque encountered at the previous trial (which is uncorrelated with the external torque at the
 current trial due to random sampling) (young 0.4139 [Nm/Nm], $\beta=1.019$, $t(53.7)=15.331$, $p<2*10^{-16}$,
 elderly 0.3915 [Nm/Nm], $\beta=0.964$, $t(30.7)=16.857$, $p<2*10^{-16}$, see Figure 3A) as well as negatively
 correlated with the planning error at the previous trial (young -0.2134 [Nm/Nm], $\beta=-0.508$, $t(58.2)=-$
 6.131, $p=8.21*10^{-8}$, elderly -0.1306 [Nm/Nm], $\beta=-0.311$, $t(34.37)=-4.283$, $p=0.000141$, see Figure 3
 B). Noteworthy is the opposite direction of these effects: While planned torques partly reflect the
 previously experienced external torque, occurring planning errors lead to a shift of the subsequent
 torque prediction to the direction of the erroneous previous prediction. Thus, the participants seemed
 to partly adhere to previous mispredictions instead of fully discarding previous sensorimotor
 prediction or even inverting them in the direction of the previous error. Although the effect of the
 planning error is highly significant in both age groups, the slopes appear to differ (see Figure 3 B)).
 However, this interaction between ‘planning error WP’ and ‘age group’ did not reach statistical
 significance ($p=0.08$). We further detected a smaller, yet highly significant, correlation with the
 external torque of the current trial (see Figure 3 C and Figure 4 C) which was included in the models
 to control for motor corrections taking place before lift onset was registered. Given our very low
 height threshold of only 0.2 mm used for lift onset detection and the subtraction of 10 ms from the
 time point at which the threshold was reached, any motor corrections before the determined moment
 of lift onset were assumed to depend on a self-imposed object-lift delay after the gravitational force
 was, at least at one object side, matched. Therefore, we hypothesized that a potential effect of the
 external torque of the current trial might interact with the time between contact and lift onset. Hence,
 we included the Z-standardized ‘contact to lift onset time’ and its interactions with ‘external torque’
 and ‘age group’ to control for the effect of Z-standardized hesitancy. Therefore, the main effect of
 ‘external torque’ (young: 0.096 [Nm/Nm], $\beta=0.236$, $t(22.6)=7.984$, $p=5.07*10^{-8}$; elderly: 0.131

[Nm/Nm], $\beta = 0.321$, $t(22.2) = 10.883$, $p = 2.31 \times 10^{-10}$) represents the effect for lifts conducted with the individual average speed. The effect increases with the individual standardized contact to lift onset time (young: 0.0335 [Nm/SD], $\beta = 0.081$, $t(2248) = 4.089$, $p = 4.48 \times 10^{-5}$; elderly: 0.0305 [Nm/SD], $\beta = 0.074$, $t(2165) = 3.991$, $p = 6.79 \times 10^{-5}$), while the interaction of the main effect with the age group just failed to achieve significance ($p = 0.055$). Elderly subjects also seemed to generate a marginally more clockwise torque with increasing time to lift onset (main effect of ‘contact to lift onset (Z-score)’ elderly: -0.0034 [Nm/SD], $\beta = -0.056$, $t(22.23) = -2.174$, $p = 0.041$). These results indicate that participants hesitated to lift the object after counteracting the gravitational force and added a small delay used for minor motor corrections in which the object was held at an undetectably low hovering state. Thus, although the measure ‘torque at lift onset’ is majorly determined by predictive processes, the motor strategy of hesitancy around the lift onset biases the measure towards the current external torque such that the real planning error is slightly underestimated.

Although the exploratory raw scatterplot (see Figure S3 D) which included a simple linear regression line hints at a linear relationship between the ‘perceived torque’ and torque planning, we found no such effect in our final model ($p = 0.52$). By controlling for the effects of the previous external torque (see also figure S5) and previous planning error which are highly correlated with the torque perception (see section 5.2), this lack of a detectable relationship implies that the conscious torque percept does not include any additional cognitive information salient to the sensorimotor system beyond the aforementioned influential variables.

In the second model the predictor ‘torque at lift onset at the previous trial’ was employed instead of the ‘external torque at the previous trial’. Hence, the main effect of the previously exerted torque at lift onset (young: 0.418 [Nm/Nm], $\beta = 0.404$, $t(32.0) = 14.66$, $p = 9.27 \times 10^{-16}$; elderly: 0.391 [Nm/Nm], $\beta = 0.378$, $t(19.4) = 15.883$, $p = 1.47 \times 10^{-12}$) represents the positive retention rate of previous

391 sensorimotor memories (see figure 4 A) and the main effect of the previous torque planning error WP
 392 (young: 0.199 [Nm/SD], $\beta = 0.472$, $t(57.3) = 5.917$, $p = 1.93 \times 10^{-7}$; elderly: 0.2507 [Nm/SD], $\beta = 0.596$,
 393 $t(32.6) = 8.596$, $p = 6.84 \times 10^{-10}$, see figure 4 B) the adaptation rate of feedback-errors in parallel to the
 394 trial-to-trial learning rule for motor adaptation (e.g. (Gonzalez Castro et al. 2014)). None of the
 395 remaining predictors not found significant in the first model reached significance, while the
 396 significant effects of the Intercept (young: -0.013 [Nm], $t(22.0) = -2.8$, $p = 0.010$); elderly: -0.018
 397 [Nm/Nm], $t(22.0) = -4.057$ [Nm], $p = 0.000525$), the current external torque (young: 0.096 [Nm/Nm],
 398 $\beta = 0.237$, $t(22.6) = 8.007$, $p = 4.83 \times 10^{-8}$; elderly: 0.130 [Nm/Nm], $\beta = 0.318$, $t(22.1) = 10.837$, $p =$
 399 2.61×10^{-10} , see Figure 4 C) and the interaction between the current external torque and the contact-to
 400 lift onset time (Z-score) (young: 0.0340 [Nm/SD], $\beta = 0.082$, $t(2254) = 4.142$, $p = 3.58 \times 10^{-5}$; elderly:
 401 0.0310 [Nm/SD], $\beta = 0.075$, $t(2164) = 4.045$, $p = 5.41 \times 10^{-5}$) as well as the negligible main effect of
 402 contact to lift onset (Z-score) in the elderly (-0.0034 [Nm/SD], $\beta = -0.056$, $t(22.19) = -2.149$, $p = 0.043$)
 403 were virtual identical to the estimates of the first model.

404 The Pseudo- R^2 of the fixed effects explains about 49.4% (I)/ 49.6% (II) of the overall variance and
 405 the random effects add an additional 12.2% (I)/ 11.5% (II) of variance explained.

406 The change in the sign of the regression coefficient of the ‘previous planning error WP’ between the
 407 two models is determined by the complimentary predictors ‘previous external torque’ in the first
 408 model and ‘previous torque at lift onset WP’ in the second model (as can be visually inferred from
 409 Figures S4 and S6). This stands in line with the deviating interpretations of the coefficients of the
 410 planning-error in the two models.

411 **5.2 Torque Perception (Z-score)**

Subjects perceived the torques according to the actual torque (young: 2.365 [SD/Nm], $\beta = 0.354$, $t(2259)=10.244$, $p < 2 \cdot 10^{-16}$; elderly: 2.743 [SD/Nm], $\beta = 0.410$, $t(2259)=13.916$, $p < 2 \cdot 10^{-16}$) and additionally to the committed planning error WP (young: 4.107 [SD/Nm], $\beta = 0.592$, $t(2259)=17.179$, $p < 2 \cdot 10^{-16}$; elderly: 3.449 [SD/Nm], $\beta = 0.497$, $t(2259)=16.765$, $p < 2 \cdot 10^{-16}$). The interaction between these two main effects ($p=0.517$) as well as the 3-way interaction with age group ($p=0.406$) were insignificant suggesting that the effects are independent from each other. The effect of the external torque was similar for both age groups ('external torque x age group' interaction: $p=0.21$), while the effect of the planning error on torque perception was smaller in the elderly group (-0.658 [SD/Nm], $\beta = -0.065$, $t(2259) = -2.086$, $p=0.037$). Remarkably, the untransformed estimates [Nm/Nm] as well as the standardized β coefficients [SD/SD] and the partial effect plots (see Figure 5) seem to convey that the committed planning errors had a stronger impact on the torque perception than the physical size of the encountered external torque, at least in the young group, while the influences rather seemed of similar strength in the elderly group.

The adjusted coefficient of model determination R^2 indicates that 82.9% of the total variance was explained by the model.

5.3 Heaviness Perception (Z-score)

On the first lift when no torque nor planning error was present (= Intercept), participants judged the object to feel significantly lighter than on their individual average (young: -0.807 [SD], $t(2282)= -14.003$, $p < 2 \cdot 10^{-16}$; elderly: -0.763 [SD], $t(2268)= -12.899$, $p < 2 \cdot 10^{-16}$). Heaviness percepts linearly increased in the course of trials (young: 0.008 [SD/trial], $\beta=0.234$, $t(2245)= 8.873$, $p < 2 \cdot 10^{-16}$; elderly: 0.008 [SD/trial], $\beta=0.234$, $t(2257)= 8.844$, $p < 2 \cdot 10^{-16}$). There was a quadratic relationship between both the external torque (main effect of External Torque²: young: 13.20[SD/Nm²], $\beta=0.267$, $t(2256)= 6.233$, $p= 1.87 \cdot 10^{-9}$; elderly: 11.991 [SD/Nm²], $\beta=0.243$, $t(1577)= 6.405$, $p= 1.65 \cdot 10^{-9}$) and

the planning error WP (main effect of Planning Error²: young: 7.532 [SD/Nm²], $\beta=0.165$, $t(2299)=3.988$, $p=6.86 \times 10^{-5}$; elderly: 7.266 [SD/Nm²], $\beta=0.159$, $t(2273)=4.722$, $p=2.48 \times 10^{-6}$), while the linear terms of these predictors were insignificant. This indicated that the minimum point of the parabola is horizontally centered at zero. None of the interactions with age reached significance. Figure 6 depicts the results.

The Pseudo-R² of the fixed effect is 19.4% with the random effects increasing the Pseudo-R² by 4.0%. This points towards a moderate overall model fit at most.

6 Discussion

The study aimed to examine the role of sensorimotor torque planning errors on the subsequent perception of object characteristics, and whether previous torque planning error, in addition to the previously encountered torque, impacted the upcoming torque planning.

6.1 Predictive Torque Control

A previous study on predictive torque exertion in uncertainty (Lukos et al. 2013) did not investigate whether previous sensorimotor model states were discarded or partly retained or even inversed according to error in the next trial in addition to updating the model state according to the encountered external torque. We hypothesized that sensorimotor memories in uncertain grasp situations do not completely decay to be overridden by last trials external torque from trial to trial, but are also partly retained. We modelled the torque prediction in two complementary ways. By selecting the previous external torque and the previous planning error as predictors in the first model, we confirmed a strong role of the previous external torque on the current torque while we could also show that subjects partly adhere to their erroneous predictions. As the externally acting torques in our experiment resemble force-field-perturbations and the exerted torques at lift onset and the planning

error can be regarded as proxies of the states of the sensorimotor memory and the feedbacked error respectively, our second model corresponds to the parameters of the trial-to-trial learning rule for motor adaptation established in force-field studies (for review see (Gonzalez Castro et al. 2014)). In accordance with that model, we found that sensorimotor memories were partly retained and partly adapted towards the occurring planning error. Whereas it takes only a few trials to learn predictive torque- (Zhang et al. 2010) or grip force- (Johansson and Westling 1988) control in real object manipulation, it takes up to 30 trials to adapt to novel force fields (Gonzalez Castro et al. 2014). In both, object torque prediction (Lukos et al. 2013) as well as force-field perturbations (Gonzalez Castro et al. 2014) the learning rates were slower when unforeseeable and repeated alterations occurred. Here, the unstandardized adaptation rates were smaller than the retention rates, while the standardized rates were of similar size. Hence, the formation of sensorimotor memories in uncertainty cannot be regarded as one-trial-learning process but as partial trial-to-trial adaptation of previous sensorimotor predictions towards experienced planning errors. As a consequence, the influence of prior trials on the current motor plan might reach further than the last trial. However, as the learning of torques normally occurs in a few trials, we expect sensorimotor carry-over- or after-effects to quickly mitigate after a few trials. Our finding that conscious sensory torque percepts did not contribute to upcoming sensorimotor torque prediction is consistent with previous studies which have shown that even explicit visual percepts of the mass distribution of an object cannot be utilized for torque prediction (Craje et al. 2013; Salimi et al. 2003).

6.2 Torque Perception

This study is the first to demonstrate that torque perception is strongly influenced in the direction of a planning error, defined as the not compensated external torque, which corresponds to the arising net torque. The regression model estimates even suggest that the effect of the planning error may be comparable or, at least in young participants, even stronger than the effect of actual external torque.

481 As we did not find evidence for an interaction between the planning error and the external torque, we
482 assume that these factors additively account for the perception of torques. Therefore, both a sensory
483 suppression of the veridical torque percept as well as sensory highlighting of the sensorimotor error
484 might underlie this perceptual bias.

485 To infer the veridical external torque, the CNS must estimate the applied compensatory torque during
486 the phase in which the object is held straight and steady after possible corrections. Therefore, the
487 CNS must integrate available sensory feedback indicating the torque. Central feed forward models of
488 action-and object dynamics are assumed to be utilized to predict the sensory consequences of planned
489 actions on the basis of a reafference copy of the motor plan (Franklin and Wolpert 2011). By
490 persistently comparing the predicted and sensed bodily states, the CNS simultaneously enhances the
491 acuity of end point estimation in reach movements (Adamovich et al. 1998; Bhanpuri et al. 2013)
492 while using forward model predictions to attenuate predicted sensory feedback caused by self-
493 generated movements (von Holst 1950). Concerning the factors relevant for our task, (Shergill et al.
494 2003) demonstrated that self-generated fingertip pressure was perceived weaker than externally
495 applied pressure of the same magnitude. While the perception of the CoP displacement was found to
496 be exaggerated when load forces diverge (Shibata et al. 2014), the active grasp-to-lift movements did
497 not alter the CoP-displacement perception compared to the perception of passively displaced CoPs
498 (Shibata et al. 2014). Hence, a possible predictive attenuation of self-generated forces resulting in
499 torques might lead to a reduced emphasis on the perception during the highly foreseeable, stable lift
500 phase in which the veridical torque can be inferred best. However, as (Craje et al. 2013) reported that
501 individuals who repeatedly lifted an object with a stable asymmetrical weight distribution judged the
502 CoM accurately, the extent of sensory attenuation in our experiment remains unclear.

When a torque planning error is made, however, this leads to a visual, proprioceptive and tactile percept of the arising rotational acceleration and object tilt which, as it was unexpected, might be attributed as having an external cause. As the initial object tilt, which is highly correlated with the planning error, is often associated with the danger of fluid spillage or loss of object control in daily life, it could be assumed that the error is particularly salient for the perceptive systems. In summary, the percept of the veridical torque during a stable object hold might be inferred by a predominantly tactile afference of well-predictable self-exerted forces, whereas the unforeseen signal arising from erroneous torque planning are probably perceived by visual, proprioceptive, and tactile inputs and experienced as externally caused. Therefore, the percept of the external torque could be exposed to predictive sensory attenuation while the planning error seem to be a sensible candidate for perceptual highlighting.

6.3 Weight Perception

Here, we sought to determine whether sensorimotor planning errors not related to weight prediction per se can also cause a weight illusion, while controlling for the influences of torques on weight perception.

Interestingly, we found that both the actual external torque as well as the planning error were quadratically related to an increase in heaviness perception. The effect of the external torque on heaviness perception stands in line with studies in which participant perceived wielded objects with more eccentric mass distributions as heavier (Amazeen and Turvey 1996). Sensorimotor errors in the adaptation of peak grip force rates prior to lift onset were recently shown to be correlated with the heaviness perception of a light object, when a heavier object was lifted before (van Polanen and Davare 2015). Here, we provide novel evidence that also not-weight related high-level sensorimotor error signals can induce misperceptions of object weight. It is worth noting that the current results, as

well as the finding of (van Polanen and Davare 2015), do not contradict the findings related to fingertip force adaptation in weight illusion studies found, where participants alternately lift objects of equal weight but differing size (Flanagan and Beltzner 2000) or material (Buckingham et al. 2009). In these studies participants were found to quickly adjust their force planning to the equal weight while continuing to judge the less heavy-looking objects to be heavier. However, while proving that the found weight illusions were not caused by sensorimotor error, the studies were not suited to examine the effect of sensorimotor errors on weight perception in a general sense as they quickly mitigated after only a few lifts.

Taken together, our findings support the theory presented by (van Polanen and Davare 2015) that both long term expectations as well as implicit, quickly learnt sensorimotor memories, shape both motor planning as well as perception. While the study designs of (Buckingham et al. 2009; Flanagan and Beltzner 2000) emphasize the impact of priors, the changes in object properties in our study and (van Polanen and Davare 2015) highlight the impact of sensorimotor prediction on weight perception. Overall the experience of object weight seems to extend beyond the veridical sensory judgment of the physical size of weight and integrates effects of violations of expectations, erroneous force prediction as well as not heaviness related object properties and planning errors

6.4 Conclusion

In summary, we provided evidence that the CNS employs feedforward predictive models to refine both upcoming motor predictions and shape the percept of object properties. While the motor system partly retained previous sensorimotor memory states and partly adapted them towards experienced errors instead of solely relying on sensory feedback, the perceptual system emphasized sensorimotor feedback leading to a perception biased in the direction of previous errors. While sensorimotor predictions impact the perception of both task-specific and unspecific object properties, no

549 contribution of conscious percepts on sensorimotor planning were detected. All major findings were
550 highly significant for both young and elderly participants.

551 **6.5 Limitations**

552 In daily object manipulation torques usually arise when objects are grasped at an eccentric handle or
553 surface, e.g. when grasping a cup or a plate. Therefore, geometric visual cues in addition to
554 sensorimotor memories guide predictive torque control and possibly also influence our object
555 perception when dealing with familiar objects. However, although less frequent, we are confronted
556 with unknown objects which conceal their mass properties, e.g. parcels. We also interact with objects
557 without looking carefully forcing us to rely more on implicit sensorimotor memories (Hesse et al.
558 2016), similar to the experimental situation in the present study. Nevertheless, the interplay of visual
559 cues, sensorimotor mechanisms and perception underlying the control of torques in daily life remains
560 to be investigated in future studies.

561 **7 Conflict of Interest**

562 The authors declare no competing financial interests.

563 **8 Acknowledgements**

564 We thank Patrick Wagner for technical assistance and Hans-Joachim Koch for his help in organizing
565 measurements.

- 567 **Aarts E, Verhage M, Veenvliet JV, Dolan CV, and van der Sluis S.** A solution to dependency:
568 using multilevel analysis to accommodate nested data. *Nat Neurosci* 17: 491-496, 2014.
- 569 **Adamovich SV, Berkinblit MB, Fookson O, and Poizner H.** Pointing in 3D space to remembered
570 targets. I. Kinesthetic versus visual target presentation. *J Neurophysiol* 79: 2833-2846, 1998.
- 571 **Amazeen EL, and Turvey MT.** Weight perception and the haptic size-weight illusion are functions
572 of the inertia tensor. *J Exp Psychol Hum Percept Perform* 22: 213-232, 1996.
- 573 **Ameli M, Dafotakis M, Fink GR, and Nowak DA.** Predictive force programming in the grip-lift
574 task: the role of memory links between arbitrary cues and object weight. *Neuropsychologia* 46: 2383-
575 2388, 2008.
- 576 **Bates D, Kliegl, R., Vasishth, S., & Baayen, H.** Parsimonious mixed models. Retrieved from
577 <http://arxiv.org/abs/150604967> 2015.
- 578 **Bates D, Mächler M, Bolker B, and Walker S.** Fitting Linear Mixed-Effects Models Using lme4.
579 *Journal of Statistical Software* 67: 1-48, 2015.
- 580 **Bates JCPDM, Pinheiro J, Pinheiro JC, and Bates D.** *Mixed-Effects Models in S and S-PLUS*.
581 Springer New York, 2000.
- 582 **Bhanpuri NH, Okamura AM, and Bastian AJ.** Predictive modeling by the cerebellum improves
583 proprioception. *J Neurosci* 33: 14301-14306, 2013.
- 584 **Breheny P, and Burchett W.** Visualization of Regression Models Using visreg. *The R Journal* 9:
585 56-71, 2017.
- 586 **Buckingham G, Cant JS, and Goodale MA.** Living in a material world: how visual cues to material
587 properties affect the way that we lift objects and perceive their weight. *J Neurophysiol* 102: 3111-
588 3118, 2009.
- 589 **Craje C, Santello M, and Gordon AM.** Effects of visual cues of object density on perception and
590 anticipatory control of dexterous manipulation. *PLoS One* 8: e76855, 2013.
- 591 **Flanagan JR, and Bandomir CA.** Coming to grips with weight perception: effects of grasp
592 configuration on perceived heaviness. *Percept Psychophys* 62: 1204-1219, 2000.
- 593 **Flanagan JR, and Beltzner MA.** Independence of perceptual and sensorimotor predictions in the
594 size-weight illusion. *Nat Neurosci* 3: 737-741, 2000.
- 595 **Flanagan JR, Wing AM, Allison S, and Spenceley A.** Effects of surface texture on weight
596 perception when lifting objects with a precision grip. *Percept Psychophys* 57: 282-290, 1995.
- 597 **Franklin DW, and Wolpert DM.** Computational mechanisms of sensorimotor control. *Neuron* 72:
598 425-442, 2011.
- 599 **Fu Q, Hasan Z, and Santello M.** Transfer of learned manipulation following changes in degrees of
600 freedom. *J Neurosci* 31: 13576-13584, 2011.
- 601 **Fu Q, and Santello M.** Context-dependent learning interferes with visuomotor transformations for
602 manipulation planning. *J Neurosci* 32: 15086-15092, 2012.
- 603 **Fu Q, Zhang W, and Santello M.** Anticipatory planning and control of grasp positions and forces
604 for dexterous two-digit manipulation. *J Neurosci* 30: 9117-9126, 2010.

605 **Gonzalez Castro LN, Hadjiosif AM, Hemphill MA, and Smith MA.** Environmental consistency
606 determines the rate of motor adaptation. *Curr Biol* 24: 1050-1061, 2014.

607 **Gordon AM, Forssberg H, Johansson RS, and Westling G.** Visual size cues in the programming
608 of manipulative forces during precision grip. *Exp Brain Res* 83: 477-482, 1991.

609 **Hermsdörfer J, Li Y, Randerath J, Goldenberg G, and Eidenmüller S.** Anticipatory scaling of
610 grip forces when lifting objects of everyday life. *Exp Brain Res* 212: 19-31, 2011.

611 **Hesse C, Miller L, and Buckingham G.** Visual information about object size and object position are
612 retained differently in the visual brain: Evidence from grasping studies. *Neuropsychologia* 91: 531-
613 543, 2016.

614 **Hoffman L.** *Longitudinal Analysis: Modeling Within-Person Fluctuation and Change*. New York:
615 Routledge, 2014.

616 **Ingram JN, Howard IS, Flanagan JR, and Wolpert DM.** A single-rate context-dependent learning
617 process underlies rapid adaptation to familiar object dynamics. *PLoS Comput Biol* 7: e1002196,
618 2011.

619 **Johansson RS, and Westling G.** Coordinated isometric muscle commands adequately and
620 erroneously programmed for the weight during lifting task with precision grip. *Exp Brain Res* 71: 59-
621 71, 1988.

622 **Johansson RS, and Westling G.** Roles of glabrous skin receptors and sensorimotor memory in
623 automatic control of precision grip when lifting rougher or more slippery objects. *Exp Brain Res* 56:
624 550-564, 1984.

625 **Kuznetsova A, Bruun Brockhoff P, and Haubo Bojesen Christensen R.** lmerTest: Tests in Linear
626 Mixed Effects Models. 2016.

627 **Lefcheck JS.** piecewiseSEM: Piecewise structural equation modeling in R for ecology, evolution,
628 and systematics. *Methods in Ecology and Evolution* 7: 573-579, 2016.

629 **Long JD.** *Longitudinal Data Analysis for the Behavioral Sciences Using R*. SAGE Publications,
630 2011.

631 **Lüdtke D.** sjstats: Statistical Functions for Regression Models. 2018.

632 **Lukos JR, Choi JY, and Santello M.** Grasping uncertainty: effects of sensorimotor memories on
633 high-level planning of dexterous manipulation. *J Neurophysiol* 109: 2937-2946, 2013.

634 **Nakagawa S, and Schielzeth H.** A general and simple method for obtaining R² from generalized
635 linear mixed-effects models. *Methods in Ecology and Evolution* 4: 133-142, 2013.

636 **R Core Team.** R: A Language and Environment for Statistical Computing. Vienna, Austria: 2018.

637 **Salimi I, Frazier W, Reilmann R, and Gordon AM.** Selective use of visual information signaling
638 objects' center of mass for anticipatory control of manipulative fingertip forces. *Exp Brain Res* 150:
639 9-18, 2003.

640 **Shergill SS, Bays PM, Frith CD, and Wolpert DM.** Two eyes for an eye: the neuroscience of force
641 escalation. *Science* 301: 187, 2003.

642 **Shibata D, Kappers AM, and Santello M.** Digit forces bias sensorimotor transformations
643 underlying control of fingertip position. *Front Hum Neurosci* 8: 564, 2014.

644 **van Polanen V, and Davare M.** Sensorimotor Memory Biases Weight Perception During Object
645 Lifting. *Front Hum Neurosci* 9: 700, 2015.

646 **von Holst EM, H.** Das Reafferenzprinzip: Wechselwirkungen zwischen Zentralnervensystem und
647 Peripherie. *Naturwissenschaften* 37: 464-476, 1950.

648 **Wickham H.** *ggplot2: Elegant Graphics for Data Analysis*. Springer-Verlag New York, 2016.

649 **Wilke CO.** cowplot: Streamlined Plot Theme and Plot Annotations for 'ggplot2'. 2017.

650 **Wolpert DM, and Flanagan JR.** Motor prediction. *Curr Biol* 11: R729-732, 2001.

651 **Wolpert DM, and Ghahramani Z.** Computational principles of movement neuroscience. *Nat*
652 *Neurosci* 3 Suppl: 1212-1217, 2000.

653 **Zhang W, Gordon AM, Fu Q, and Santello M.** Manipulation after object rotation reveals
654 independent sensorimotor memory representations of digit positions and forces. *J Neurophysiol* 103:
655 2953-2964, 2010.

656 **Zwislocki JJ, and Goodman DA.** Absolute scaling of sensory magnitudes: a validation. *Percept*
657 *Psychophys* 28: 28-38, 1980.

658 **10 Figures**

659 Figure 1: Experimental setup. The custom-built grip-device consists of a handle element mounted
660 centrally on a horizontal bar (A, B). The handle element allowed subjects to freely choose digit
661 placement on the sandpaper (Bosch, P320) covered grasp surfaces (40 x 120mm) (A). The aluminum
662 panels underneath the surfaces were mounted on 6-axis-force/torque sensors and blocked the sensors
663 from view (The panels are rendered transparent for illustrative purposes in B). A magnetic position/
664 orientation tracker was mounted centrally on the horizontal bar (A). A 250g aluminum weight was
665 randomly placed into the 5 cavities of the horizontal bar. The hereby resulting horizontal positions of
666 the center of mass and the external torques arising after lift onset in the vertical object orientation are
667 denoted in B. The orange circle denotes the center of mass of the grip device with the aluminum
668 weight placed in the right cavity (B). A detachable lid blocked the cavities from view (A). To
669 indicate their perception of the center of mass/ the external torque, subjects used the needle of a
670 digital caliper which was parallel to the horizontal bar and aligned with the right edge of the grip
671 device (A).

672 Figure 2: Representative trial illustrating the task variables. The upwards directed load force sum
673 (LF) exceeds the gravitational force prior to object lift onset (thick vertical line). The mean grip force
674 (GF) acting orthogonal towards the grasp surfaces causes friction preventing finger slip. In order to
675 prevent object tilt, the total exerted torque must compensate for the external torque (horizontal
676 dashed line in the torques subplot) which is depicted for the moment of lift onset with a perfectly
677 vertical object orientation. For the calculation of the exerted torque see supplementary Figure S1. The
678 planning error denotes the difference between the external torque and the exerted torque at lift onset,
679 hence the uncompensated- or net torque at lift onset and is envisaged as vector pointing from the
680 exerted torque at lift onset towards the external torque. The planning error is highly correlated with
681 the peak object tilt occurring in the first 300 ms after lift onset (thin dashed vertical line).

682 Figure 3: Partial effects plots of the significant main effects of the first linear mixed effects
683 regression model for the exerted torque at lift onset with 95% prediction intervals of the effects
684 computed by parametric bootstrapping and partial residuals. The effects are separately plotted for
685 both age groups. As the external torque has discrete values, we display the distribution of the data
686 with box and whiskers plots in the style of Tukey. The central horizontal line represents the median,
687 while the lower and upper hinges correspond to the 25th and 75th percentiles, respectively. The
688 upper and lower whiskers extend from the upper and lower hinge to the largest value no further
689 than $1.5 \times$ inter-quartile ranges from the respective hinges. Data beyond are plotted individually.
690 Additionally, the means are indicated by a 'X'.

691 Figure 4: Partial effects plots of the significant main effects of the second linear mixed effects
692 regression model for the exerted torque at lift onset with 95% prediction intervals of the effects
693 computed by parametric bootstrapping and the partial residuals. The effects are separately plotted for
694 both age groups. As the external torque has discrete values, we display the distribution of the data
695 with box and whiskers plots in the style of Tukey with additional 'X' denoting the means.

696 Figure 5: Partial effects plots of the significant main effects of the multiple linear regression model
697 for the perceived torque with 95% prediction intervals and the partial residuals. The effects are
698 separately plotted for both age groups. As the external torque has discrete values, we display the
699 distribution of the data with box and whiskers plots in the style of Tukey with additional 'X'
700 denoting the means.

701 Figure 6: Partial effects plots of the significant main effects of the linear mixed effects regression
702 model for the perceived weight with 95% prediction intervals of the effects computed by parametric
703 bootstrapping and the partial residuals. The effects are separately plotted for both age groups. As the

704 external torque has discrete values, we display the distribution of the data with box and whiskers
705 plots in the style of Tukey with additional 'X' denoting the means.

11 Supplementary Material

Figure S1: Task mechanics. Panel A illustrates the forces ‘F’ exerted on the object in a 3-finger tripod grip, with the left hand with the subscript ‘ind’ denoting the index finger, ‘mi’ the middle finger and ‘th’ the thumb. The registered torques around the z-axis of the F/T-Sensors T_{zi} result from the sum of the product of the load force F_{yi} of the respective side and the distance between the grasp surface and the sensor surface a ($a=2.4$ mm) and the product of the grip force of the respective side F_{xi} and the vertical CoP_i relative to the sensor reference point: $T_{zi} = a * F_{yi} + CoP_i * F_{xi}$. Therefore, the center of pressure (CoP) relative to the sensor reference point in the center of each sensor surface can be calculated as: $CoP_i = \frac{T_{zi} - a * F_{yi}}{F_{xi}}$. Panel B depicts the external and exerted torques acting on the object around an axis which goes through the center between the F/T-sensors parallel to the z-axis and the variables necessary for calculation. The external torque $T_{external}$ arising at lift onset is caused by the mass asymmetry of the object and is equivalent to the product of the gravitational force vector of the device F_{Gtotal} and the horizontal center of mass CoM_h : $T_{external} = F_{Gtotal} * CoM_h$. As a convention, we denote clockwise external torques and compensating counter clockwise exerted torques as positive. The exerted torque is comprised of two components: (1) the product of the side difference between the load forces ΔLF ($\Delta LF = F_{y_{right}} - F_{y_{left}}$) and half the distance between the grasp-surfaces $w/2$ ($w/2 = 20$ mm): $T_{tangential} = \frac{w}{2} * \Delta LF$; (2) the product of the grip forces of each side which can be approximated as equal $F_{x1} \approx F_{x2} \approx GF_{mean}$ and the difference of the vertical positions of the CoPs between the grasp sides ΔCoP ($\Delta CoP = CoP_{right} - CoP_{left}$): $T_{CoP*GF} = \Delta CoP * GF_{mean}$. Hence, the total exerted torque equals: $T_{exerted} = \frac{w}{2} * \Delta F_y + \Delta CoP * GF_{mean}$.

Figure S2: Exerted torques at lift onset plotted against trial per age group with overlaid group-wise ‘loess’- regression lines and density lines of the distributions. Evidently, the torque at lift onset was

728 scaled to a similar degree across trials and age groups. The exerted torques at lift onset fluctuated
729 around a marginally clockwise average torque, presumably due to the majorly right handedness of the
730 subjects. Horizontal dashed lines indicate the maximal external torques which had to be compensated
731 for (± 0.21 Nm).

732 Figure S3: Scatterplots of the exerted torque at lift onset plotted against A) the external torque at the
733 previous trial, B) the planning error WP at the previous trial, C) the external torque at the current
734 trial, D) the perceived torque (Z-score) at the previous trial and E) the exerted torque at lift onset at
735 the previous trial. Distinct plots for both age groups are presented. As the external torque has discrete
736 values, we display the distribution of the data with box and whiskers plots in the style of Tukey. The
737 central horizontal line represents the median, while the lower and upper hinges correspond to the
738 25th and 75th percentiles, respectively. The upper and lower whiskers extend from the upper and
739 lower hinge to the largest value no further than $1.5 \times$ inter-quartile ranges from the respective hinges.
740 Data beyond are plotted individually. Additionally, the means are indicated by a 'X'. The subplots
741 contain simple linear regression lines for illustrative purposes which do not correspond to the
742 inferential multiple regression model results and the partial effect plots depicted in Figure 3 and 4.

743 Figure S4: Scatterplots of the exerted torque at lift onset plotted against the previous planning error
744 WP, plotted separately by the previous external torque and the age group. The subplots contain
745 simple linear regression lines for illustrative purposes. For each previous external torque, the torque
746 at lift onset is negatively correlated with the previous planning error.

747 Figure S5: Scatterplots of the exerted torque at lift onset plotted against the previous perceived
748 torque (Z-score), plotted separately by the previous external torque and the age group. The subplots
749 contain simple linear regression lines for illustrative purposes. Controlling for the previous external

750 torque, there seems to be no obvious correlation of the torque at lift onset with the previous torque
751 percept (Z-score).

752 Figure S6: Three-dimensional Scatterplots of the Torque at lift onset plotted against A) the previous
753 planning error and the previous external torque and B) the previous planning error and the previous
754 exerted torque at lift onset. The scatterplots contain linear regression surfaces based on the regression
755 with the two respective predictors for illustrative purposes. The values of the torque at lift onset are
756 color coded. While A) depicts a negative correlation between the torque at lift onset with the previous
757 planning error while controlling for the previous external torque, the correlation is positive in B)
758 when controlling for the effect of the previous exerted torque at lift onset instead.

759 Figure S7: Indicated and actual center of mass (CoM) plotted across trials for each participant. The
760 inner-dashed lines represent the actual range of the CoM, the outer-dashed lines the full caliper range
761 which fully spans the object's base. Evidently, participants considerably differed in the range of their
762 estimates. Participant 4 seemed to alternately indicate positions on the left and the right, irrespective
763 of the actual CoM and was therefore removed from further analysis.

764 Figure S8: Perceived torques at lift onset plotted against trial per age group with overlaid 'loess'-
765 regression lines and density lines of the distributions. The perceived torques evenly fluctuate around
766 zero. Interestingly the distribution of the torque percepts seems to be trimodal in both age groups.

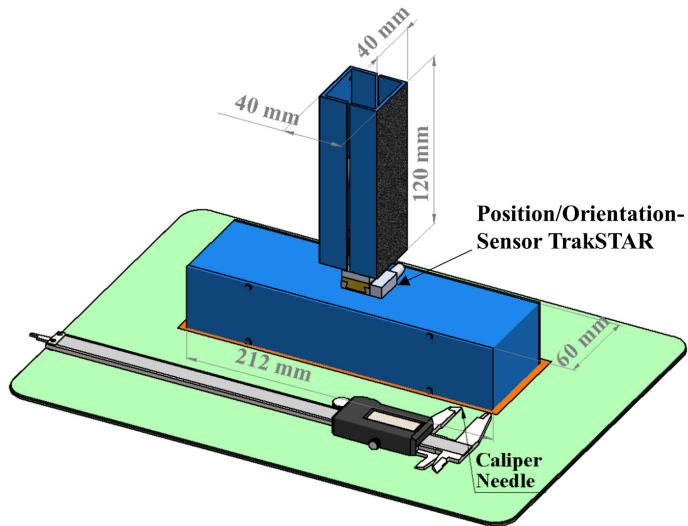
767 Figure S9: Scatterplots of the perceived torque (Z-score) plotted against the planning error WP,
768 plotted separately by the external torque and the age group. The subplots contain simple linear
769 regression lines for illustrative purposes which do not correspond to the inferential multiple
770 regression model results and the partial effect plots depicted in Figure 5.

771 Figure S10: Weight ratings (Z-scores) plotted against trial per age group with overlaid 'loess'-
772 regression lines and density lines of the distributions. Several subjects perceived the heaviness as
773 outlying low during the very first trials. After the first trials the percepts seem to evenly fluctuate
774 across trials with the non-parametric regression line suggesting a linear increase across trials. The
775 distribution of the percepts is comparable in both age groups. Horizontal dashed lines indicate ± 2.5 ,
776 ± 2 and ± 1 SDs.

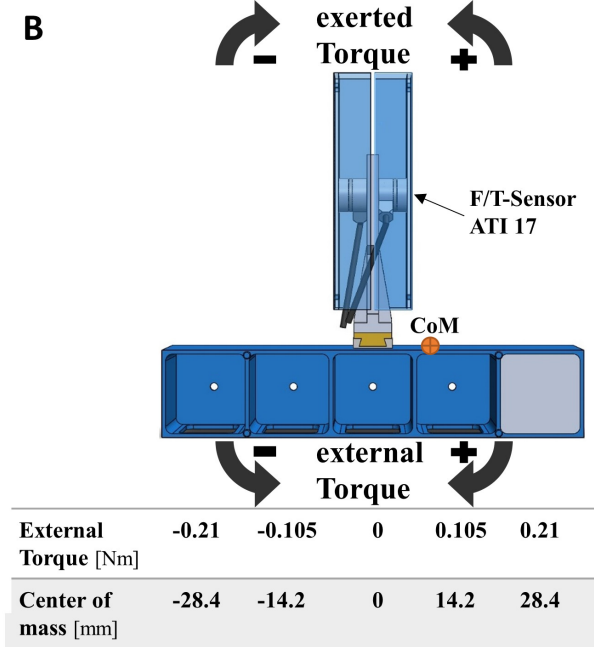
777 Figure S11: Scatterplots of the perceived weight (Z-score) plotted against A) the external torque and
778 B) the planning error WP. As the external torque has discrete values, we display the distribution of
779 the data with box and whiskers plots in the style of Tukey with additional 'X' denoting the means
780 The subplots plots contain non-parametric 'loess'-regression lines for illustrative purposes which do
781 not correspond to the inferential multiple regression model results and the partial effect plots depicted
782 in Figure 6.

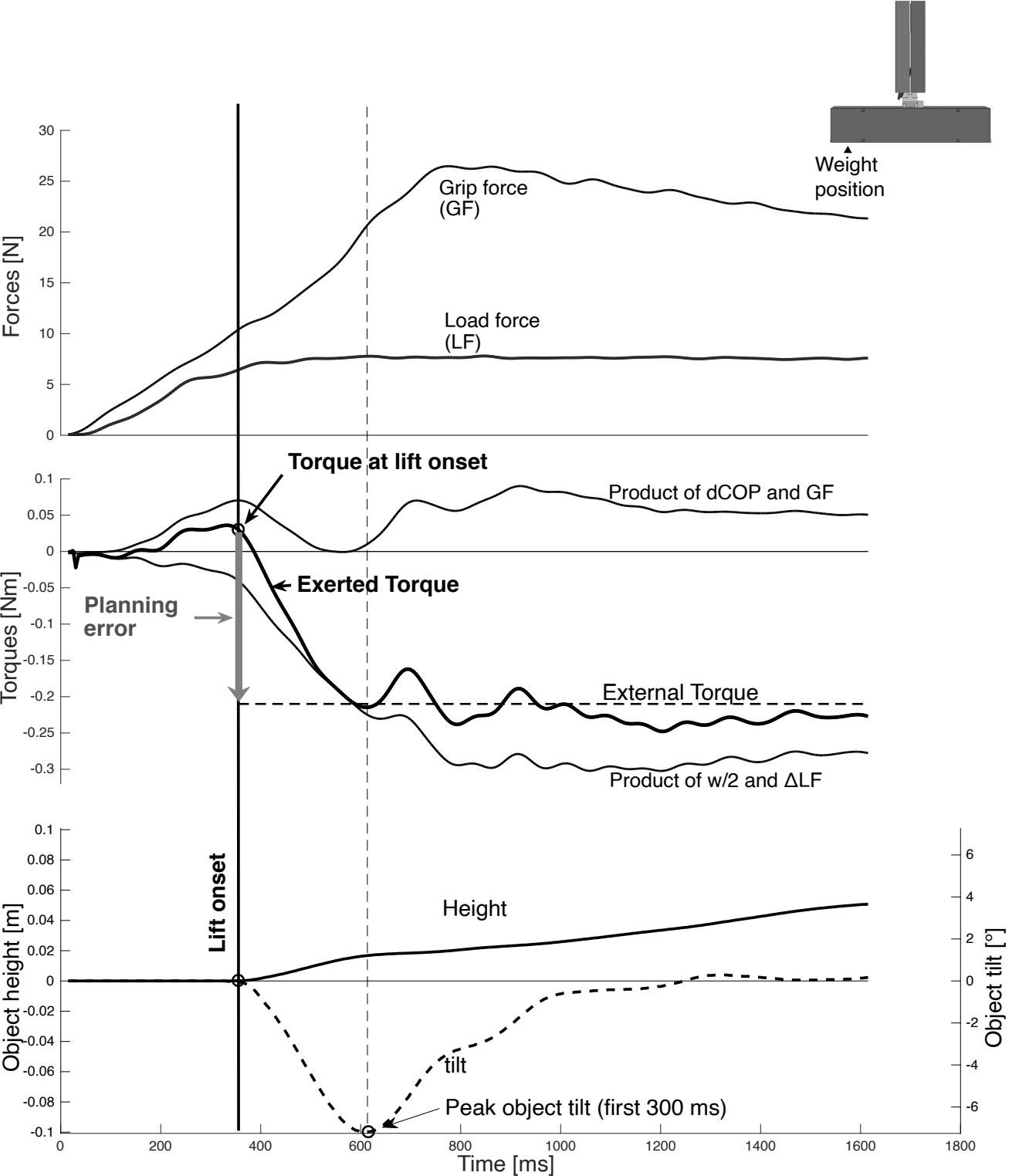
783

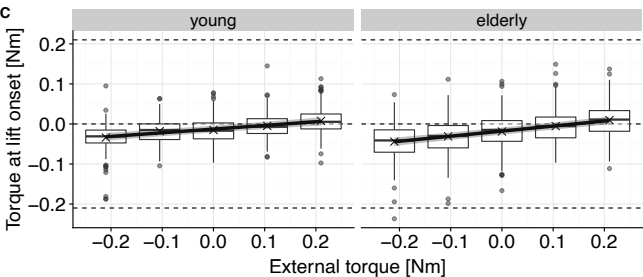
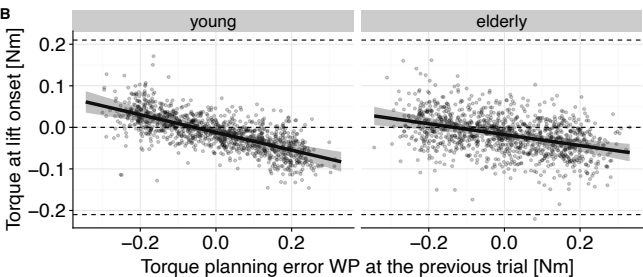
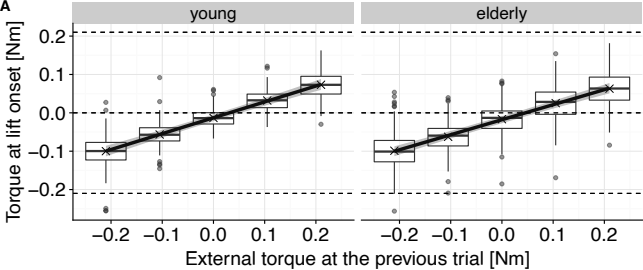
A

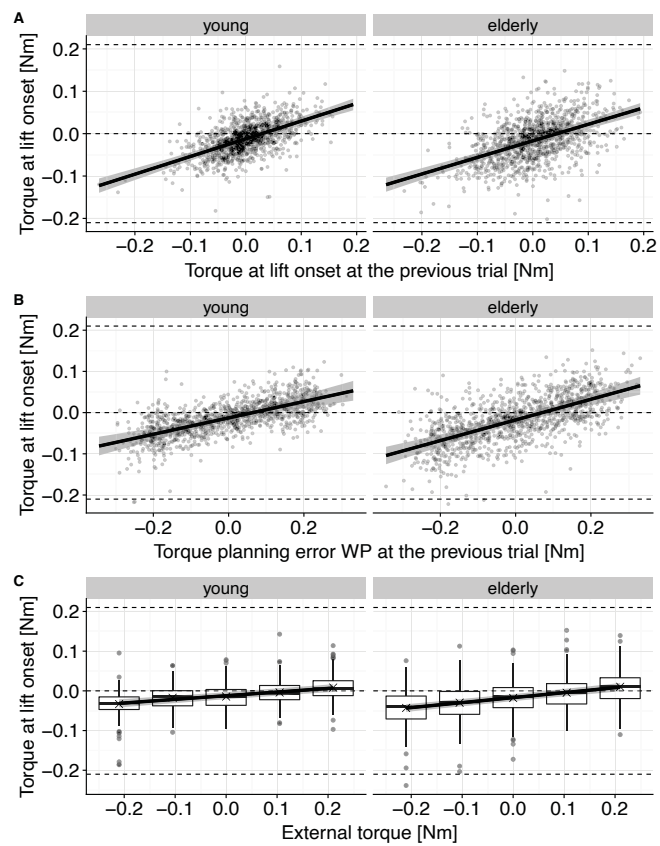


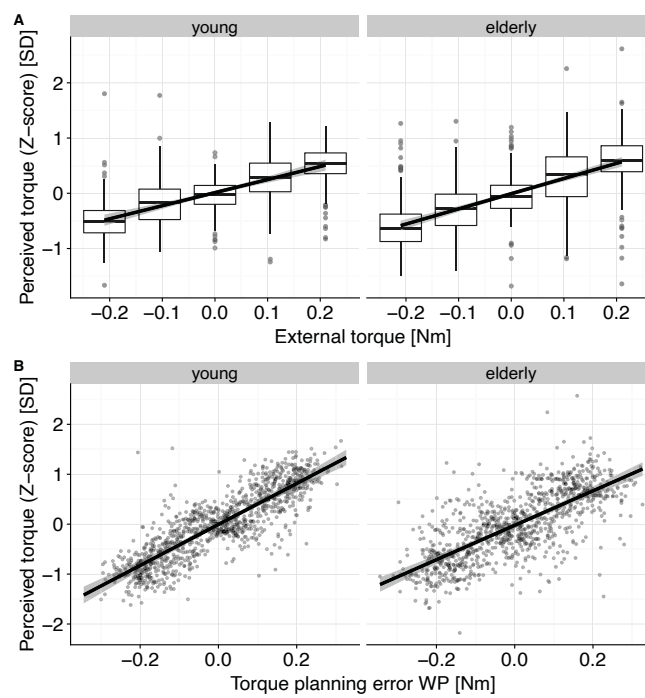
B

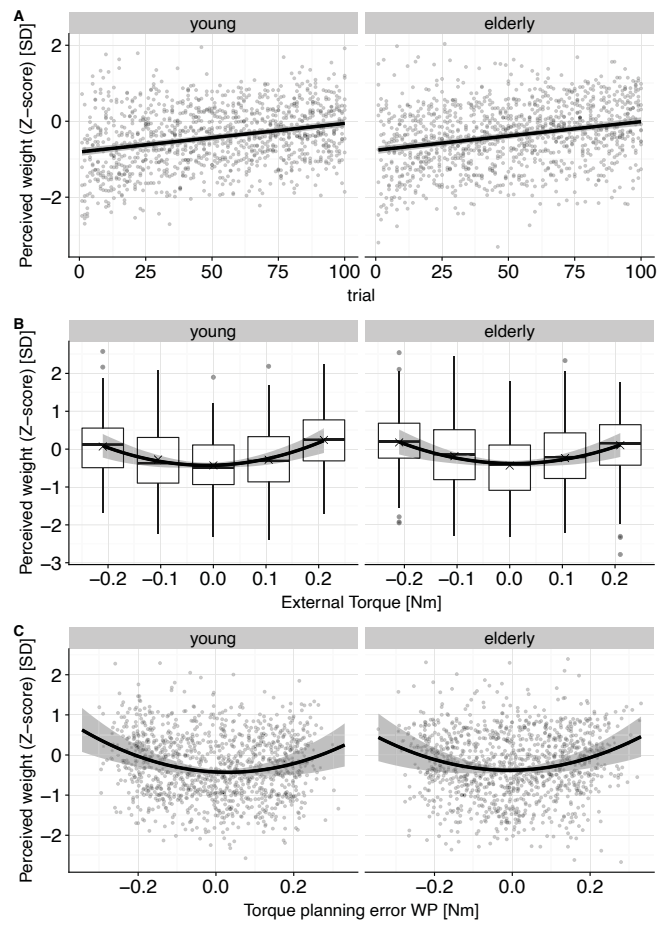




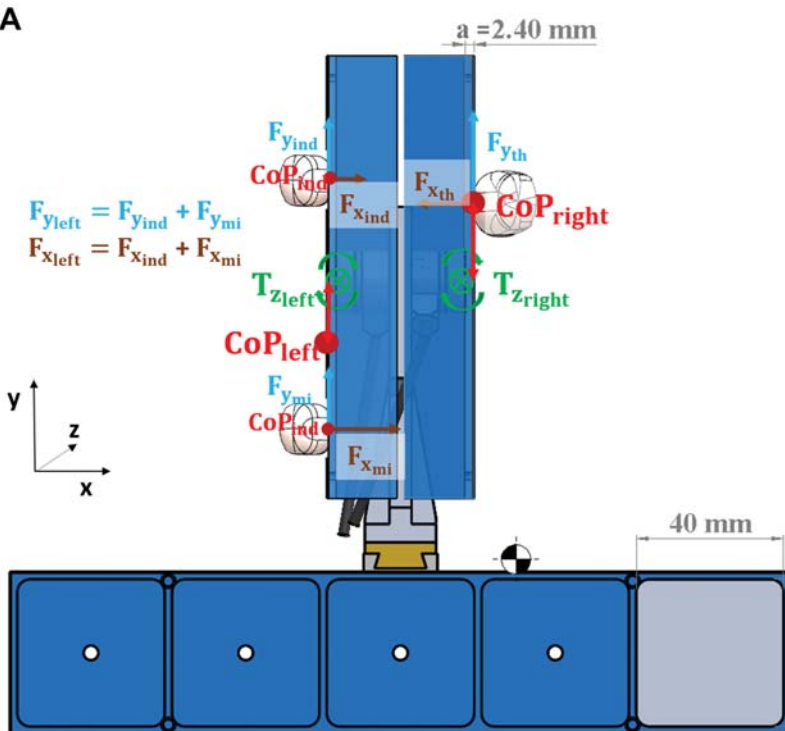




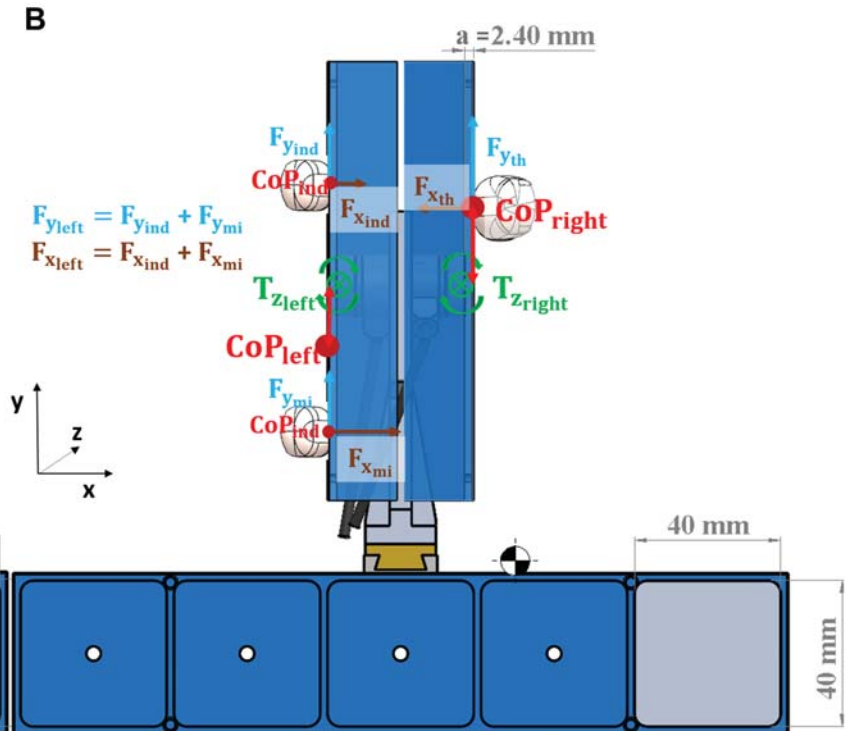


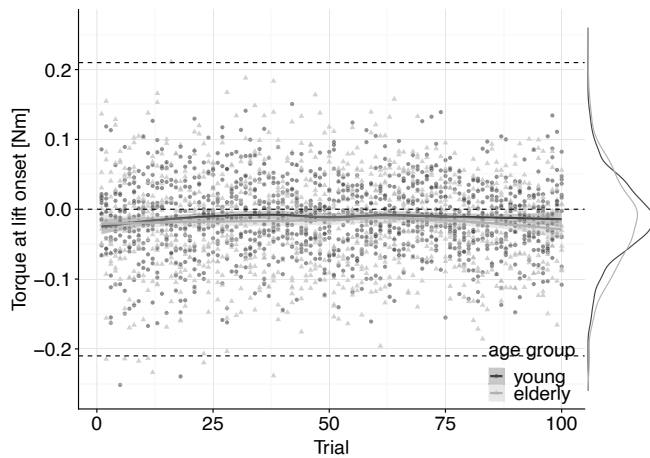


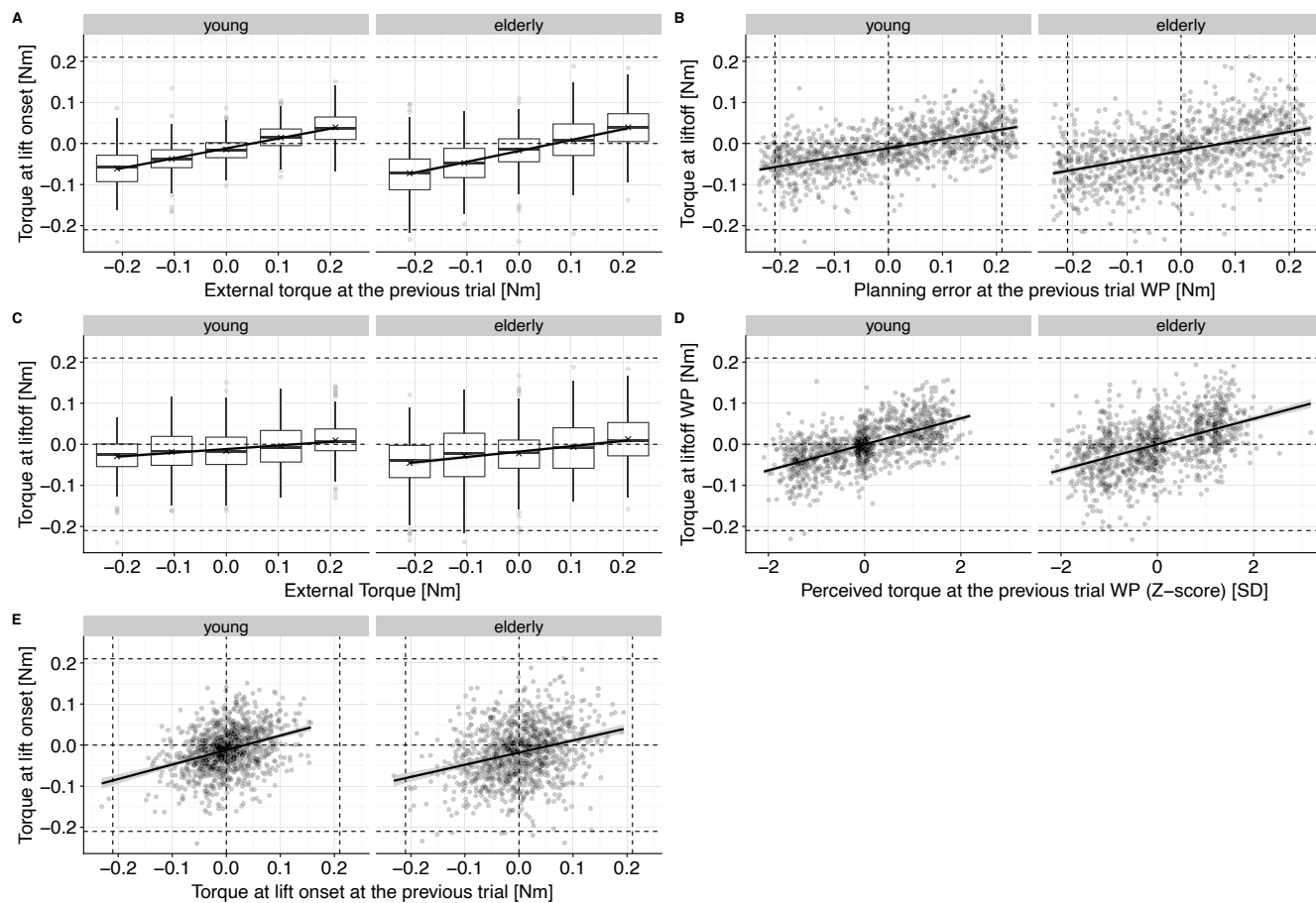
A

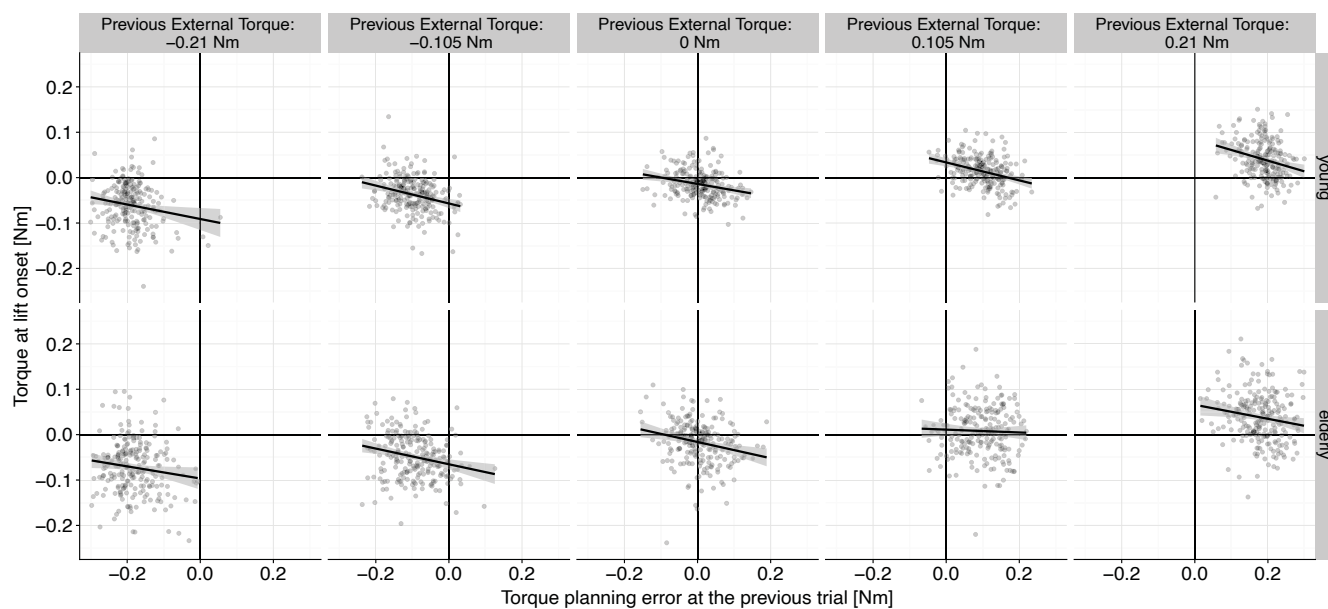


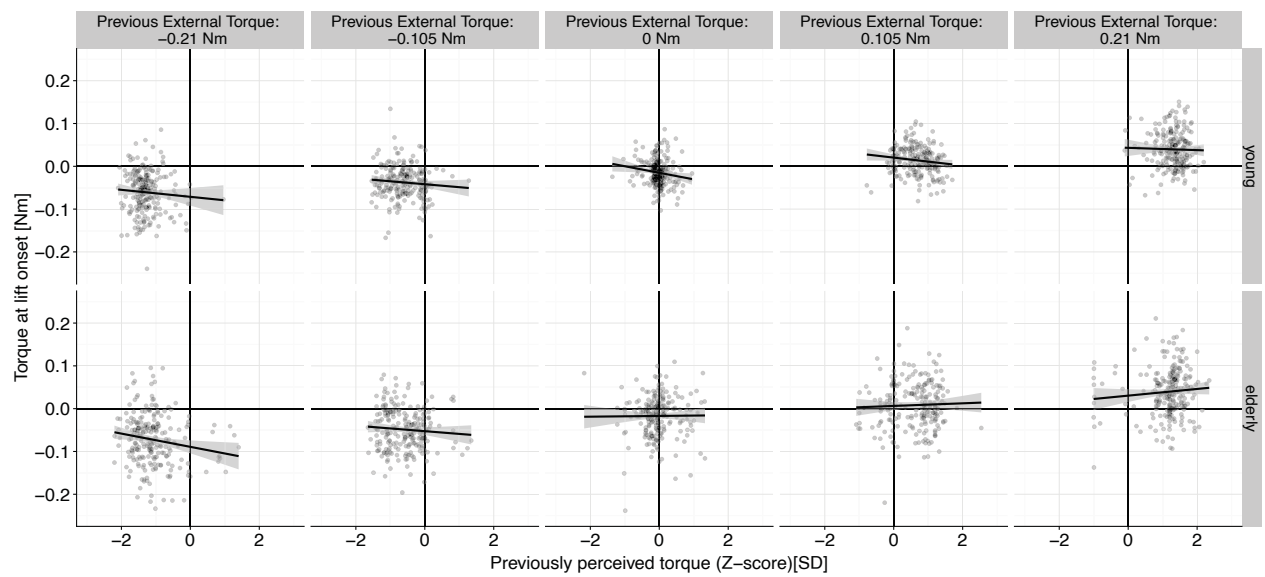
B

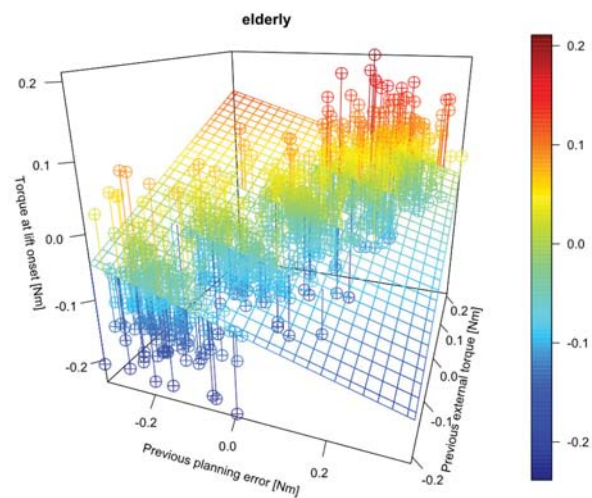
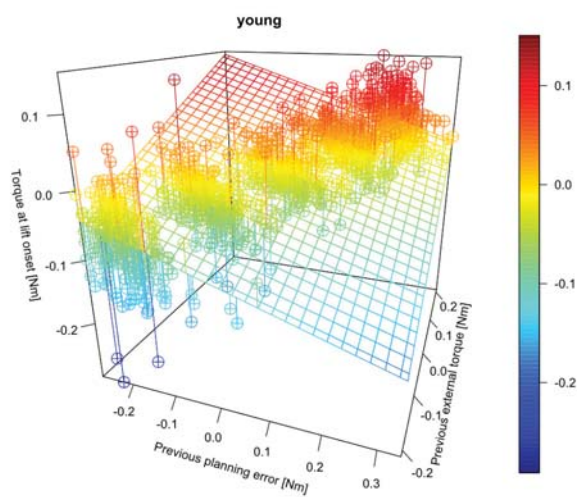
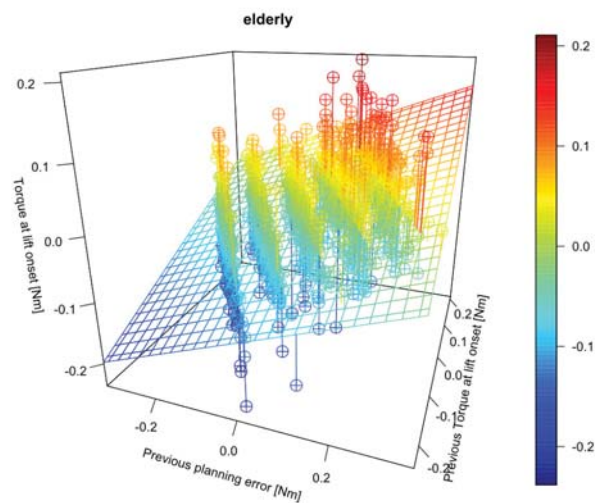
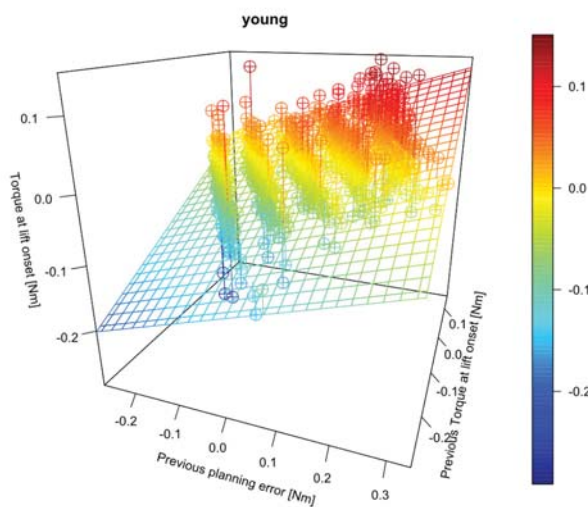


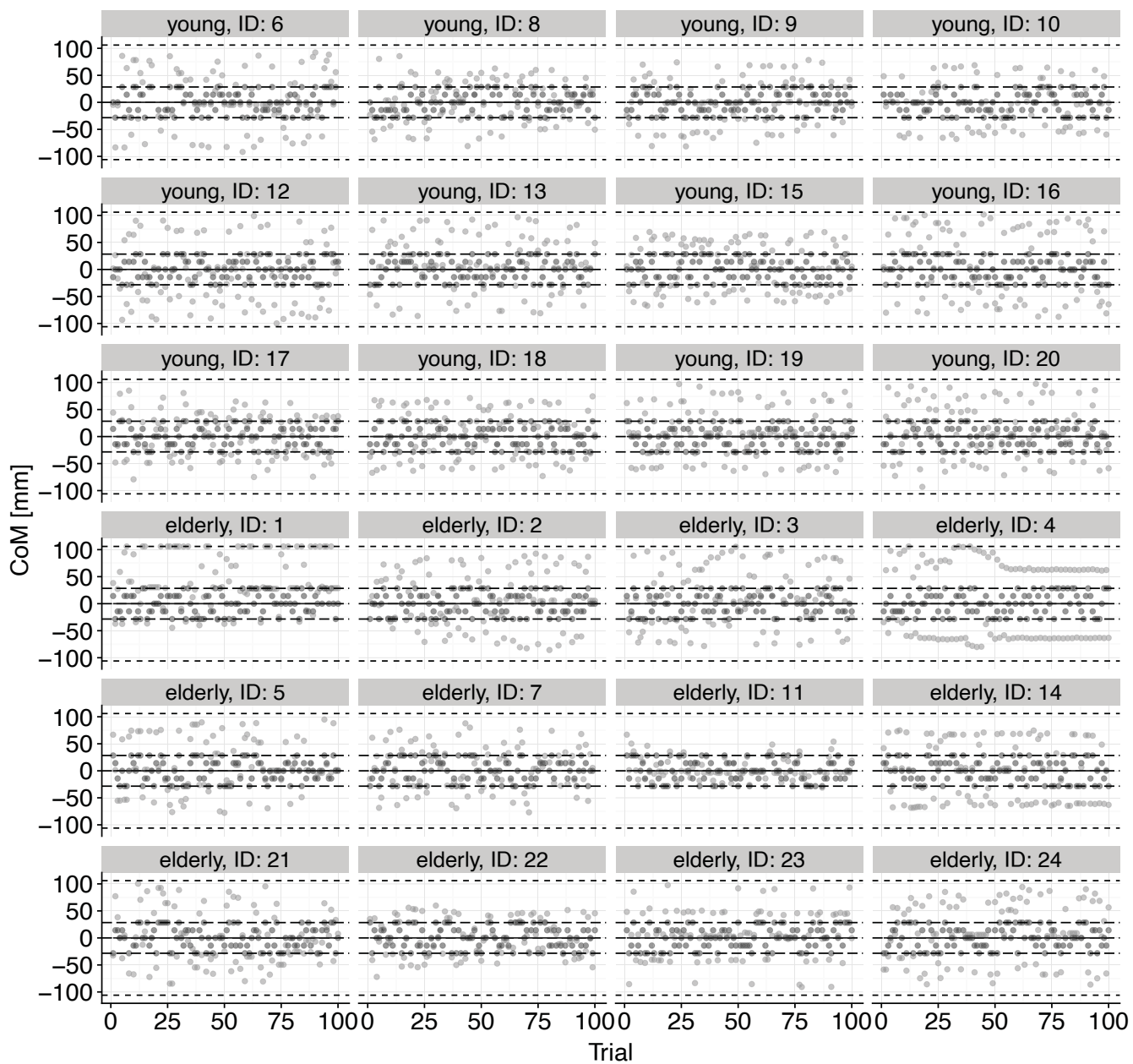








A**B**



• Actual CoM • Indicated CoM

